Greenwood, C., & Wilson, M. T. (1971) *Eur. J. Biochem. 22*, 5–10.
Lin, L.-N., & Brandts, J. F. (1983a) *Biochemistry 22*, 559–563.
Lin, L.-N., & Brandts, J. F. (1983b) *Biochemistry 22*, 1430–1437.
Looze, Y., Polastro, E., Gielens, C., & Leonis, J. (1976) *Biochem. J. 157*, 773–775.
Margoliash, E., & Frohwirt, N. (1959) *Biochem. J. 71*, 570–572.
Motonaga, K., Misaka, E., Nakajima, E., Ueda, S., & Nakanishi, K. (1965a) *J. Biochem. (Tokyo) 57*, 22–28.
Motonaga, K., Katano, H., & Nakanishi, K. (1965b) *J. Biochem. (Tokyo) 57*, 29–33.
Myer, Y. P. (1968a) *Biochemistry 7*, 765–776.
Myer, Y. P. (1968b) *J. Biol. Chem. 243*, 2115–2122.
Nall, B. T., & Landers, T. A. (1981) *Biochemistry 20*, 5403–5411.
Narita, K., & Titani, K. (1969) *J. Biochem. (Tokyo) 65*, 259–267.
Polastro, E., Looze, Y., & Leonis, J. (1976) *Biochim. Biophys. Acta 446*, 310–320.
Ridge, J. A., Baldwin, R. L., & Labhardt, A. M. (1981) *Biochemistry 20*, 1622–1630.
Schellman, J. A. (1978) *Biopolymers 17*, 1305–1322.
Stellwagen, E., & Babul, J. (1975) *Biochemistry 14*, 5135–5140.
Takano, T., Trus, B. L., Mandel, N., Mandel, G., Kallai, O. B., Swanson, R., & Dickerson, R. E. (1977) *J. Biol. Chem. 252*, 775–785.
Wilson, M. T., Ranson, R. J., Masiakowski, P., Czarnecka, E., & Brunori, M. (1977) *Eur. J. Biochem. 77*, 193–199.
Yaoi, Y. (1967) *J. Biochem. (Tokyo) 61*, 54–58.
Zuniga, E. H., & Nall, B. T. (1983) *Biochemistry 22*, 1430–1437.

# Redox Chemistry of Sulfide-Bridged Derivatives of the Binuclear Iron Site in Hemerythrin from *Phascolopsis gouldii*†

Gudrun S. Lukat and Donald M. Kurtz, Jr.*
*Department of Chemistry, Iowa State University, Ames, Iowa 50011*
*Received November 6, 1984*

ABSTRACT: Reported are redox potentials and redox chemistry for the binuclear iron site of hemerythrin (Hr), when bridging $S^{2-}$ is substituted for bridging $O^{2-}$ (or $OH^-$). The sulfide-bridged derivatives can be reversibly cycled between the met and semi-met oxidation levels, $\mu$-$S^{2-}$met and $\mu$-$S^{2-}$semi-met, respectively, at pH 8.0. The midpoint reduction potentials for this couple are in the range of 283–312 mV vs. NHE and depend on the presence or absence of perchlorate. $\mu$-$S^{2-}$met slowly autoreduces to $\mu$-$S^{2-}$semi-met in anaerobic solutions. The autoreduction, which consistently occurs to the extent of 80–85%, can be explained in terms of the successive reactions $\mu$-$S^{2-}$met → met + $S^{2-}$ and $S^{2-}$ + $\mu$-$S^{2-}$met → $\mu$-$S^{2-}$semi-met + $SO_3^{2-}$. The reactions of both $\mu$-$S^{2-}$met and $\mu$-$S^{2-}$semi-met with $O_2$ are sulfide based and result in met- and semi-metHr, respectively. The latter reaction appears to proceed through $(\text{semi-met})_O$. $O_2$ appears to react with bound $S^{2-}$, since the reactions with $O_2$ are much faster than anaerobic dissociation of $S^{2-}$. Unlike $O_2$, ligand anions accelerate the autoreduction of $\mu$-$S^{2-}$met. This acceleration causes the reaction of $\mu$-$S^{2-}$met with $O_2$ in the presence of $N_3^-$ to proceed through $\mu$-$S^{2-}$semi-met. Perchlorate slows both oxidative loss of sulfide and autoreduction. $\mu$-$S^{2-}$semi-met cannot be reduced by $S_2O_4^{2-}$; however, electron paramagnetic resonance evidence indicates that $S^{2-}$ apparently does interact with deoxyHr. From the observation that $S^{2-}$ substitutes at the semi-met but not at the met oxidation level, a $\mu$-hydroxo bridge is proposed to bridge the iron atoms in semi-metHr. Lack of stable anion adducts of $\mu$-$S^{2-}$met or $\mu$-$S^{2-}$semi-met suggests severe steric restrictions at both oxidation levels. The ~200-mV positive shift in met/semi-met reduction potential when bridging $O^{2-}$ is replaced by bridging $S^{2-}$ is consistent with hard–soft acid–base theory. The potentials of the $\mu$-$S^{2-}$met/$\mu$-$S^{2-}$semi-met couple fall within the range of "Rieske"-type [2Fe-2S] centers. It is proposed that histidine imidazoles provide some of the ligands to the iron atoms in the Rieske center.

The non-heme oxygen-carrying protein hemerythrin (Hr)[1] occurs in certain marine invertebrates, most commonly as an octamer of $M_r$ 108 000. Each of the eight identical subunits contains a binuclear iron site. Upon oxygenation this binuclear site is converted from a form containing two high-spin $Fe^{2+}$ ions (deoxyHr) to a form containing two high-spin $Fe^{3+}$ ions with the bound dioxygen reduced to the peroxide oxidation state (oxyHr) (Kurtz et al., 1977; Sanders-Loehr & Loehr, 1979; Wilkins & Harrington, 1983; Klotz & Kurtz, 1984). DeoxyHr and oxyHr can be oxidized to a form containing two high-spin $Fe^{3+}$ ions per site, which no longer reversibly binds $O_2$ (metHr). This form does bind a number of small anions, hereafter referred to as ligand anions.

† This research was supported by National Science Foundation Grant PCM-8216447.

[1] Abbreviations: Hr, hemerythrin; EPR, electron paramagnetic resonance; Tris, tris(hydroxymethyl)aminomethane; $metN_3^-$, semi-$metN_3^-$, and $deoxyN_3^-$, azide adducts of met-, semi-met-, and deoxyHr, respectively; $\mu$-$S^{2-}$met and $\mu$-$S^{2-}$semi-met were previously identified as $metS^{2-}$ and semi-$metS^{2-}$, respectively (Lukat et al., 1984).

0006-2960/85/0424-3464$01.50/0 

Chart I

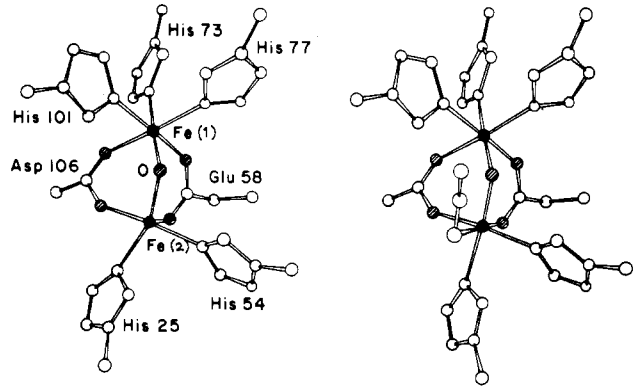


Methemerythrin ($Fe^{3+}/Fe^{3+}$) Azidomethemerythrin ($Fe^{3+}/Fe^{3+}/N_3^-$)

The geometry of the iron site in metHr and that of the azide adduct ($metN_3^-$) both determined by X-ray crystallography are shown in Chart I (Stenkamp et al., 1983, 1984). The iron atoms are separated by ~3.3 Å. Recent results show that $O_2$ in oxyHr occupies the same coordination site as does $N_3^-$ in $metN_3^-$ (Stenkamp et al., 1985). In both oxy- and metHrs the $\mu$-oxo bridge induces antiferromagnetic coupling between the iron atoms leading to a diamagnetic ground state (Dawson et al., 1972). One-electron reduction of metHr yields an intermediate oxidation level known as $(semi\text{-}met)_R$ in which a high-spin $Fe^{2+}$ and a high-spin $Fe^{3+}$ are coupled in a single site. The spectroscopy and reactivity of $(semi\text{-}met)_R$ differ from those of the alternate form, $(semi\text{-}met)_O$, which is obtained by one-electron oxidation of deoxyHr (Bradić et al., 1980; Babcock et al., 1980). $^1H$ NMR studies indicate that the degree of antiferromagnetic coupling is reduced by about 1 order of magnitude in $semi\text{-}metN_3^-$ compared to $metN_3^-$ (Maroney et al., 1984). The coupling in semi-metHr induces an $S = {}^1/_2$ ground state, which leads to characteristic EPR spectra for $(semi\text{-}met)_O$, $(semi\text{-}met)_R$, and their ligand anion adducts (Muhoberac et al., 1980; Harrington et al., 1982).

A sulfide derivative of Hr was first reported in 1965 (Keresztes-Nagy & Klotz, 1965). On the basis of resonance Raman spectra of this derivative, Freier et al. (1979) suggested that a $\mu$-sulfido bridge had replaced the $\mu$-oxo bridge. We have shown that this sulfide derivative is at the semi-met oxidation level having an $S = {}^1/_2$ ground state similar to that of other semi-metHrs (Kurtz et al., 1983). More recently, we reported that this semi-metsulfideHr ($\mu$-$S^{2-}$semi-met) can be one-electron oxidized to a met form ($\mu$-$S^{2-}$met), whose properties are consistent with retention of the bridging sulfide (Lukat et al., 1984). Introduction of sulfide has a marked effect on the physical and chemical properties of the iron site in Hr. Some of these new properties resemble those of [2Fe-2S] centers in ferredoxins. These include accessibility of only $Fe^{3+}Fe^{3+}$ and $Fe^{3+}Fe^{2+}$ oxidation levels having $S = 0$ and $S = {}^1/_2$ ground states, respectively, and trapped valence irons in the reduced form (Kurtz et al., 1983). Herein we report the redox chemistry of the $\mu$-$S^{2-}$Hrs and compare this chemistry with that of the $\mu$-oxo-containing forms as well as with that of [2Fe-2S] sites in iron–sulfur proteins.

## Experimental Procedures

OxyHr was isolated and crystallized from the coelomic fluid obtained from live worms of the species *Phascolopsis gouldii* purchased from Marine Biological Laboratories, Woods Hole, MA (Klotz, et al., 1957). MetHr was prepared by dialysis of solutions of oxyHr against 50 mM Tris–perchlorate or Tris–acetate, pH 8.0, containing $K_3Fe(CN)_6$. Excess ferricyanide was then removed by dialysis. DeoxyHr was prepared by anaerobic dialysis at 4 °C of oxyHr against 2–3 mM $Na_2S_2O_4$ followed by dialysis against 50 mM Tris–acetate, pH 8.0, to remove excess $Na_2S_2O_4$. $(Semi\text{-}met)_O$ was prepared by addition of 1 equiv of $K_3Fe(CN)_6$ to deoxyHr.

*Preparation of $\mu$-$S^{2-}$met.* All operations were carried out at 4 °C under $N_2$ or Ar unless noted otherwise. MetHr was dialyzed against 3–5 mM $Na_2S{\cdot}9H_2O$ in 50 mM Tris–acetate (or perchlorate), pH 8.0, for ~10 h. The resulting $\mu$-$S^{2-}$ semi-met was transferred to the appropriate buffer containing 3–4 mM $K_3Fe(CN)_6$ and dialyzed for ~10 h. The resulting $\mu$-$S^{2-}$met if not used immediately was frozen and stored in liquid $N_2$. Samples of $\mu$-$S^{2-}$met were passed over a Sephadex G-25 column to remove excess $Fe(CN)_6^{3-/4-}$ immediately before use. Protein concentrations expressed as monomer were determined spectrophotometrically with published extinction coefficients for $\mu$-$S^{2-}$met (Lukat et al., 1984).

*Preparation of $\mu$-$S^{2-}$semi-met.* MetHr was dialyzed against sulfide as described above, and excess sulfide was removed either by anaerobic dialysis or by centrifugation through a small Sephadex G-25 column. Alternatively, 1 reducing equiv of $Na_2S_2O_4$ was added to $\mu$-$S^{2-}$met. Concentrations of stock solutions of $Na_2S_2O_4$ were determined by titration with $K_3Fe(CN)_6$ solutions whose concentrations were determined with $\epsilon_{420} = 1030\ M^{-1}\ cm^{-1}$ (Irwin et al., 1983). The $\mu$-$S^{2-}$semi-met concentration was determined with $\epsilon_{500} = 1100\ M^{-1}\ cm^{-1}$ (Freier et al., 1979).

*Measurements of Midpoint Reduction Potentials of the $\mu$-$S^{2-}$met/$\mu$-$S^{2-}$semi-met Couple. (A) Using $Fe(CN)_6^{3-}/Fe(CN)_6^{4-}$.* All measurements were made anaerobically at pH 8.0 and 25 °C. Keeping the total concentration of $Fe(CN)_6^{3-}$ plus $Fe(CN)_6^{4-}$ constant at either 40 or 80 mM, anaerobic solutions containing various ratios of $K_3Fe(CN)_6$ to $K_4Fe(CN)_6$ were prepared in either 50 mM Tris–acetate or 50 mM Tris–perchlorate, pH 8.0, containing 50 mM $Na_2SO_4$. A value of $E^0 = 430$ mV vs. NHE was used for the $Fe(CN)_6^{3-}/Fe(CN)_6^{4-}$ couple (O'Reilly et al., 1973). These conditions are close to those used by Armstrong et al. (1983) in determinations of the $(semi\text{-}met)_O$/deoxyHr reduction potential. Concentrated (1–3 mM) solutions of either $\mu$-$S^{2-}$met or $\mu$-$S^{2-}$ semi-met were added to the $Fe(CN)_6^{3-}/Fe(CN)_6^{4-}$ solutions resulting in total protein concentrations of 0.10–0.16 mM. Relative concentrations of $\mu$-$S^{2-}$met and $\mu$-$S^{2-}$semi-met at equilibrium were determined from absorbances at 500 and 544 nm. Each $Fe(CN)_6^{3-}/Fe(CN)_6^{4-}$ solution was background corrected against a $Fe(CN)_6^{4-}$ stock solution before addition of protein. Least-squares analyses of data points from three to six titrations were used to generate the lines from which the midpoint potentials were extracted. Further details are given in the tables and figure legends.

*(B) Using Cytochrome c.* Oxidized horse heart cytochrome *c* ($Fe^{3+}$cyt *c*) (Sigma type III) was used. Ferrocytochrome *c* ($Fe^{2+}$cyt *c*) was obtained from $Fe^{3+}$cyt *c* either by dialysis against or direct addition of dithionite. Cytochrome *c* concentrations were determined by visible absorbances at 550 and 528 nm ($\epsilon_{550} = 29.5\ mM^{-1}\ cm^{-1}$ for $Fe^{2+}$cyt *c*, $\epsilon_{550} = 9.0\ mM^{-1}\ cm^{-1}$ for $Fe^{3+}$cyt *c*, and $\epsilon_{528} = 11.2\ mM^{-1}\ cm^{-1}$ for $Fe^{3+}$cyt *c*) (Margoliash & Frohwirt, 1959; Margoliash & Walasek, 1967). The reactions of $\mu$-$S^{2-}$met with $Fe^{2+}$cyt *c* and of $\mu$-$S^{2-}$semi-met with $Fe^{3+}$cyt*c* were monitored at 550 nm. All initial protein concentrations were 0.11 mM. Spectrophotometric determinations of [$\mu$-$S^{2-}$met] and [$\mu$-$S^{2-}$semi-met] at equilibrium were impossible due to the intense absorbance of cyt *c*. Therefore, these concentrations were estimated by

Scheme I

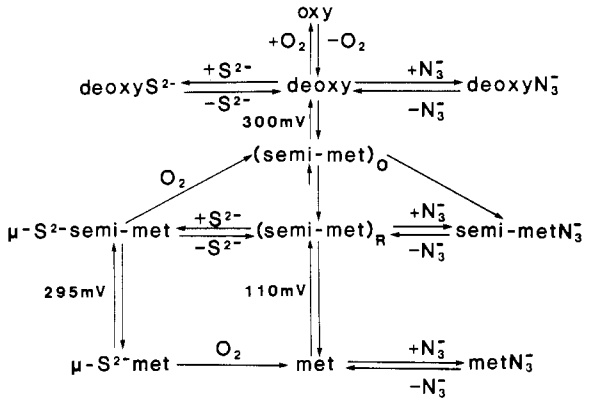


double integration of $\mu$-$S^{2-}$semi-met EPR spectra. An $E^0$ of 0.26 V vs. NHE was used for cytochrome *c* (Margalit & Schejter, 1973; Heineman et al., 1975). This value was also used by Armstrong et al. (1983).

*Reactions with Ligand Anions and Dioxygen.* Stock solutions of reagent-grade commercial samples of sodium salts of azide, nitrite, chloride, thiocyanate, cyanide, and fluoride were used. In reactions of the $\mu$-$S^{2-}$Hrs with $O_2$, stirred solutions were left open to air at room temperature. No attempts were made to add known quantities of $O_2$.

*Spectroscopy.* Absorption spectra were obtained on a Perkin-Elmer Model 554 spectrophotometer. Anaerobic samples were placed in double septum sealed quartz cuvettes, which were similar to a previous design (Averill et al., 1978). EPR spectra were obtained on 0.1-mL aliquots of reaction mixtures contained in 4 mm o.d. quartz tubes, which were evacuated and flame sealed after freezing the samples in liquid nitrogen. X-band spectra were obtained on a Bruker Model ER220D spectrometer equipped with an Oxford ESR-10 helium flow system. Copper sulfate was used as the concentration standard for areas obtained by double integration (Aasa & Vänngard, 1975).

## Results and Discussion

Scheme I summarizes the results of this investigation, which are discussed in detail below. The reduction potentials cited for the met/$(semi\text{-}met)_R$ and $(semi\text{-}met)_O$/deoxy couples are those determined by Armstrong et al. (1983). Although evidence for some aspects of Scheme I was presented previously, the present work extends, clarifies, and justifies Scheme I.

*Midpoint Reduction Potentials of the $\mu$-$S^{2-}$met/$\mu$-$S^{2-}$semi-met Couple.* Measurements of the reduction potentials made use of equilibrium 1. For this one-electron redox process

$$\mu\text{-}S^{2-}\text{met} + Fe(CN)_6^{4-} \rightleftarrows \mu\text{-}S^{2-}\text{semi-met} + Fe(CN)_6^{3-} \quad (1)$$

in the presence of a large excess of $Fe(CN)_6^{3-/4-}$, the solution potential ($E_{soln}$) is determined by the $Fe(CN)_6^{3-}/Fe(CN)_6^{4-}$ ratio. Simple Nernstian considerations show that a plot of $E_{soln}$ vs. log ([$\mu$-$S^{2-}$met]/[$\mu$-$S^{2-}$semi-met]) should yield a straight line with a slope of 59 mV, and the midpoint potential where log ([$\mu$-$S^{2-}$met]/[$\mu$-$S^{2-}$semi-met]) = 0 is the standard reduction potential under the conditions employed. Such plots determined under various conditions are shown in Figure 1, and the midpoint potentials are listed in Table I. The slopes in Figure 1 are all 59 ± 1 mV, confirming the one-electron nature of the process. Equilibration under our conditions takes ~15 min.

The reactions of equimolar concentrations of $\mu$-$S^{2-}$met with $Fe^{2+}$cyt *c* and of $\mu$-$S^{2-}$semi-met with $Fe^{3+}$cyt *c* give identical visible absorption spectra at equilibrium, which was attained

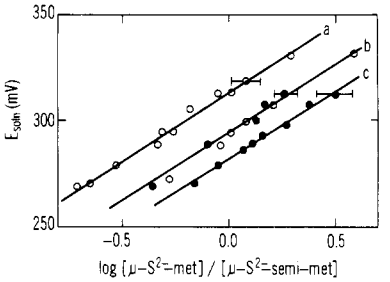


FIGURE 1: Plots of $E_{soln}$ vs. log ([$\mu$-$S^{2-}$met]/[$\mu$-$S^{2-}$semi-met]). Data points are each the average of values obtained from three separate redox titrations using $A_{544}$ to measure [$\mu$-$S^{2-}$met] and [$\mu$-$S^{2-}$semi-met]. Conditions were as follows: 0.13–0.14 mM Hr; pH 8.0; $I$ = 0.15 M; 25 °C. Open circles represent titrations starting from $\mu$-$S^{2-}$semi-met; filled circles represent titrations starting from $\mu$-$S^{2-}$met. Data points for lines a and c were obtained in 50 mM Tris–acetate; data points for line b were obtained in 50 mM Tris–perchlorate.

Table I: Midpoint Reduction Potentials ($E_m$) for the $\mu$-$S^{2-}$met/$\mu$-$S^{2-}$semi-met Couple at 25 °C, $I$ = 0.15 M, and pH 8.0[a]

| conditions | $E_m$ (mV) vs. NHE[b] | redox partner |
|---|---|---|
| m or sm ($ClO_4^-$)[c] | 295 ± 5 | $Fe(CN)_6^{4-/3-}$ |
| m ($OAc^-$) | 283 ± 8 | $Fe(CN)_6^{4-/3-}$ |
| sm ($OAc^-$) | 312 ± 5 | $Fe(CN)_6^{4-/3-}$ |
| m ($ClO_4^-$) | 287 ± 25[d] | $Fe^{2+}$cyt *c*/$Fe^{3+}$cyt *c* |

[a] In 50 mM Tris buffer with the counterion listed in parentheses at ~25 mM. [b] Each value represents the average from three to six separate redox titrations (see Figure 1). [c] m and sm refer to titrations starting from $\mu$-$S^{2-}$met (m) or $\mu$-$S^{2-}$semi-met (sm). In Tris–acetate this notation also refers to the conformers of Scheme II (see text). [d] Average of six titrations.

Scheme II

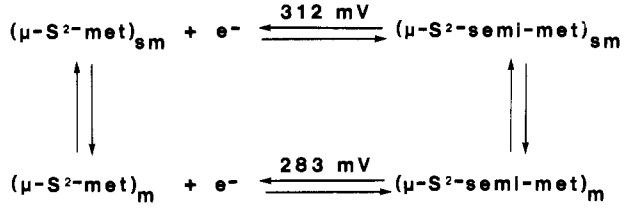


in 30–45 min. Concentrations of $\mu$-$S^{2-}$semi-met and $Fe^{3+}$cyt *c* determined from double integration of their respective EPR spectra (which do not overlap each other) coupled with the $Fe^{3+}/Fe^{2+}$cyt *c* reduction potential, $E^{0\prime}$ = 260 mV (Margalit & Schejter, 1973), allow calculation of a value for the $\mu$-$S^{2-}$met/$\mu$-$S^{2-}$semi-met reduction potential (Table I). The value obtained with the cyt *c* couple, although less precise, is in very good agreement with that obtained by the $Fe(CN)_6^{3-/4-}$ equilibration method. The lower precision is due to the larger uncertainty in the concentrations obtained from integrations of EPR spectra rather than optical spectra. The value reported is the average obtained from six independent equilibration experiments.

As can be seen from Figure 1 and Table I a single value for the reduction potential is obtained starting from either $\mu$-$S^{2-}$met or $\mu$-$S^{2-}$semi-met in Tris–perchlorate whereas a 29-mV difference is obtained in Tris–acetate. This latter difference can be rationalized in terms of two conformers. When either $\mu$-$S^{2-}$met or $\mu$-$S^{2-}$semi-met is prepared in Tris–acetate as described under Experimental Procedures, the resulting conformation is that which stabilizes either the met or semi-met oxidation level. We designate these conformers in Scheme II as m and sm, respectively. Relative to the time scale of the redox titrations (15–30 min), the vertical equilibria shown in Scheme II must be slow in order that the conformational differences be reflected in the midpoint potentials.

One must also assume that $S_2O_4^{2-}$ (acting as $SO_2^{-}\cdot$ perhaps in an inner sphere fashion) but not $Fe(CN)_6^{4-}$ (acting in an outer sphere fashion) can induce the conformational change m → sm. One possible explanation for the lower potential of the m conformer is that it has a higher affinity for the negatively charged $Fe(CN)_6^{3-/4-}$. In this case the midpoint potential should depend on the total concentration of $Fe(CN)_6^{3-/4-}$ (Dutton & Wilson, 1974). However, the midpoint potential starting from $\mu$-$S^{2-}$met in Tris–acetate was found to be the same (within 8 mV) when measured by total $Fe(CN)_6^{3-/4-}$ concentrations of either 40 or 80 mM.

Assuming the existence of two conformers, the effect of perchlorate can be rationalized as a stabilization of the sm conformer, such that the same midpoint potential is obtained starting from either direction (Figure 1). The decrease from 312 to 295 mV would then be due predominantly to the electrostatic effect of bound $ClO_4^-$ (Burkey & Gross, 1982). X-ray diffraction results on *Themiste dyscritum* Hr show that perchlorate binds to the surface of the protein and causes slight structural changes at or near the iron site (Stenkamp et al., 1978, 1983, 1984). Perchlorate is known to lower the rate of ligand anion binding to *P. gouldii* metHr and to raise the $pK_a$ of the protein from 7.8 to 8.7 (Bradić et al., 1983; Darnall et al., 1968; Garbett et al., 1971). Perchlorate also slows the rate of autoreduction of *P. gouldii* $\mu$-$S^{2-}$met (Lukat et al., 1984). These observations suggest that upon binding of $ClO_4^-$ a single conformer is stabilized starting from either $\mu$-$S^{2-}$met or $\mu$-$S^{2-}$semi-met.

Only slight differences are observed in the EPR spectra of $\mu$-$S^{2-}$semi-met prepared in Tris–acetate vs. Tris–perchlorate. However, as discussed below, oxidative loss of $S^{2-}$ from $\mu$-$S^{2-}$semi-met results in an EPR spectrum resembling that of $(\text{semi-met})_O$. It is thus tempting to associate the sm conformer with $(\text{semi-met})_O$ and the m conformer with $(\text{semi-met})_R$. We have no evidence linking the two conformers of the $\mu$-$S^{2-}$Hrs with acidic and basic forms of the iron sites, such as occurs in metHr (Bradić & Wilkins, 1983). Both EPR and optical spectra of the $\mu$-$S^{2-}$Hrs remain essentially constant between pH 6.5 and pH 9.5. Whatever the explanation for the range of values, the significant result is that replacement of the $\mu$-oxo by a $\mu$-sulfido bridge in Hr results in an ~200-mV increase in the met/semi-met reduction potential (Scheme I). This increase is most likely due predominately to intrinsic differences in potential of the iron sites rather than conformational differences between Hr and $\mu$-$S^{2-}$Hr. Comparing potentials of what appear to be similar conformers, i.e., those of met/$(\text{semi-met})_R$ and $(\mu\text{-}S^{2-}\text{met})_m/(\mu\text{-}S^{2-}\text{semi-met})_m$, gives a 173-mV increase.[2] An intrinsic increase in potential is reasonable on the basis of hard–soft acid–base theory.

*Anaerobic Stabilities of the $\mu$-$S^{2-}$Hrs.* $\mu$-$S^{2-}$semi-met is stable anaerobically at 4 °C for several weeks if excess $S^{2-}$ is present. Removal of $S^{2-}$ by extended anaerobic dialysis at 4 °C results in a solution giving a mixture of $(\text{semi-met})_O$ and/or $(\text{semi-met})_R$ and $\mu$-$S^{2-}$semi-met EPR signals. A mixture of these signals is seen even after anaerobic dialysis of $\mu$-$S^{2-}$semi-met for 20 days at 4 °C, although the major contribution appears to be from $(\text{semi-met})_R$ in this case (spectra not shown). Little or no reduction in overall EPR intensity occurs during these dialyses. We have confirmed by monitoring of EPR spectra the observation by Freier et al. (1979) that no reaction occurs when excess $N_3^-$ is added to $\mu$-$S^{2-}$semi-met under anaerobic conditions at room temperature.

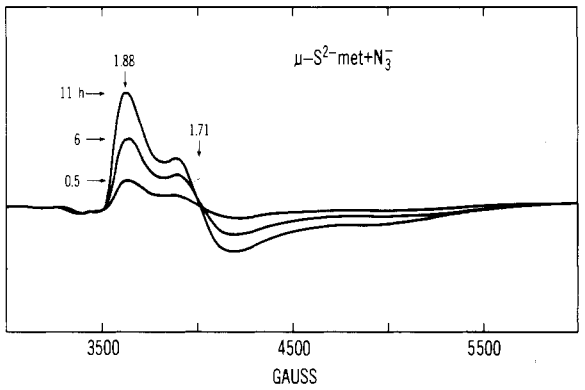


FIGURE 2: EPR spectra observed during anaerobic incubation at room temperature of 1.48 mM $\mu$-$S^{2-}$met in 50 mM Tris–acetate, pH 8.0, in the presence of 0.84 mM $NaN_3$. EPR conditions were as follows: temperature 4 K; frequency 9.569 GHz; power 101 $\mu$W; modulation amplitude 16G at 100 kHz; time constant 0.2 s; receiver gain $5.0 \times 10^4$. Double integration gives the following spins per two Fe (time): 0.07 (0.5 h), 0.5 (6 h), and 0.85 (11 h). Times are listed in order of increasing intensity at $g = 1.88$.

We have previously reported that $\mu$-$S^{2-}$met slowly autoreduces in anaerobic solutions and that the $\mu$-$S^{2-}$semi-met EPR signal is the only one seen during autoreduction (Lukat et al., 1984). In light of the rather positive reduction potentials reported above, this autoreduction is not surprising. As mentioned above, the autoreduction is substantially slower in the presence of perchlorate. At room temperature the first signs of the $\mu$-$S^{2-}$semi-met EPR signal in Tris–acetate, pH 8.0, are observed after 12 h with the maximum $\mu$-$S^{2-}$semi-met concentration (0.82 spin per two Fe) being detected after 48 h. In Tris–perchlorate, pH 8.0, no EPR signal is seen before 44 h, and the maximum signal (0.81 spin per two Fe) is seen at 80 h. On the basis of primarily these spin quantitations, we propose that this autoreduction consists of reactions 2 and

$$\mu\text{-}S^{2-}\text{met} + H_2O \rightarrow \text{met} + HS^- + H^+ \quad (2)$$

3. Theoretically, only 14.3% of $S^{2-}$ needs to dissociate via

$$6\mu\text{-}S^{2-}\text{met} + HS^- + 3H_2O \rightarrow 6\mu\text{-}S^{2-}\text{semi-met} + SO_3^{2-} + 7H^+ \quad (3)$$

reaction 2 to reduce the remaining 85.7% of $\mu$-$S^{2-}$met to $\mu$-$S^{2-}$semi-met via reaction 3, which is consistent with the experimental spin quantitations. On the basis of our measured potentials for the reduction of $\mu$-$S^{2-}$met to $\mu$-$S^{2-}$semi-met (283–312 mV) and the sulfite/sulfide reduction potential ($E^{0\prime}$ = −120 mV) (Krueger & Siegel, 1982), reaction 3 is thermodynamically feasible.[3]

The autoreduction of $\mu$-$S^{2-}$met (reactions 2 and 3) is accelerated in the presence of ligand anions. Although ligand anions do not form stable adducts of $\mu$-$S^{2-}$met (Lukat et al., 1984), they could conceivably cause dissociation of the bridging sulfide in $\mu$-$S^{2-}$met by "attack" of ligand anion at the 5-coordinate iron. The increased rate of autoreduction can thus be viewed as an acceleration of reaction 2 by ligand anion. Due

[2] Since metHr is presumed to exist only in the R conformation (Babcock et al., 1980), there is no value known for a "$(\text{met})_O/(\text{semi-met})_O$" potential to our knowledge. As illustrated in Figure 6, the $(\text{semi-met})_O \rightleftarrows (\text{semi-met})_R$ equilibrium clearly lies toward $(\text{semi-met})_R$ for *P. gouldii* Hr. Thus, in this case the reduction potential for met/$(\text{semi-met})_O$ must be less positive than the value for met/$(\text{semi-met})_R$ of 110 mV.

[3] Our anaerobic titrations of metHr with sulfide, when followed spectrophotometrically, require ~1.2 $S^{2-}$ per two Fe to reach $\mu$-$S^{2-}$semi-met quantitatively. Theoretically, the consecutive reactions 6met + $HS^-$ + $3H_2O$ → 6semi-met + $SO_3^{2-}$ + $7H^+$ and semi-met + $S^{2-}$ → $\mu$-$S^{2-}$semi-met would require 1.17 $S^{2-}$ per two Fe. We detect no reaction of either met or $\mu$-$S^{2-}$met with $Na_2SO_3$.

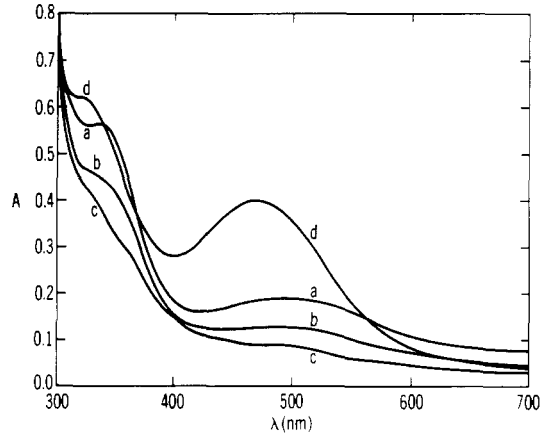


FIGURE 3: Absorption spectra obtained during aerobic incubation of 0.16 mM $\mu$-$S^{2-}$semi-met in 50 mM Tris–acetate, pH 8.0, at room temperature. Cell path length = 1 cm. Reaction times were as follows: (a) immediately after removal of excess sulfide by passage over a Sephadex G-25 column; (b) 25 min; (c) 115 min; (d) after addition of $NaN_3$ at 150 min.

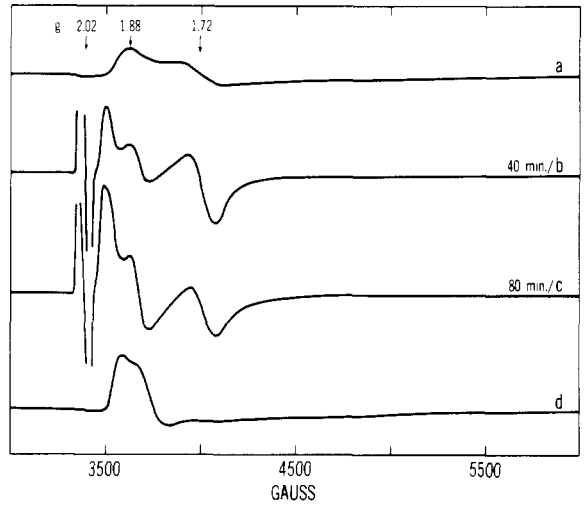


FIGURE 4: EPR spectra observed during incubation of 1.95 mM $\mu$-$S^{2-}$semi-met in 50 mM Tris–acetate, pH 8.0, at room temperature: (a) before exposure to air; (b and c) after exposure to air for the indicated times; (d) after addition of excess $N_3^-$ to sample in (c). Sample in (c) had been passed over a Sephadex G-25 column before freezing. EPR conditions are those listed in the legend to Figure 2 except the frequency is 9.750 GHz.

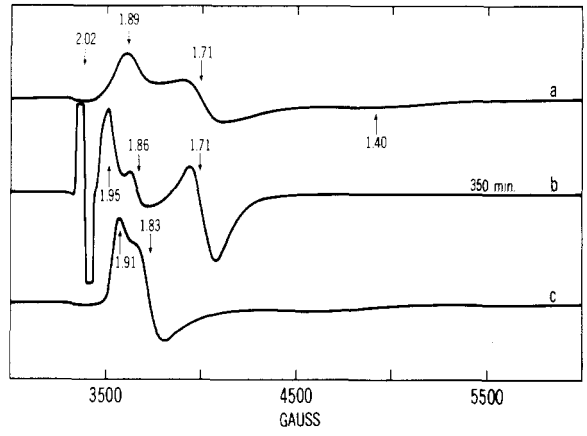


FIGURE 5: EPR spectra observed during aerobic incubation of 1.94 mM $\mu$-$S^{2-}$semi-met in 50 mM Tris–perchlorate, pH 8.0, at room temperature: (a) immediately after removal of excess $S^{2-}$ by passage over a Sephadex G-25 column; (b) after 350-min exposure to air; (c) after addition of $NaN_3$ to 0.515 M at 345-min exposure to air. EPR conditions are those listed in the legend to Figure 4.

to tight binding of azide to metHr, the autoreduction in this case should theoretically result in 14.3% met$N_3^-$ and 85.7% $\mu$-$S^{2-}$semi-met. Starting with $\mu$-$S^{2-}$met in Tris–acetate anaerobically at room temperature, addition of an ~570-fold excess of azide results in the maximum $\mu$-$S^{2-}$semi-met concentration (0.85 spin per two Fe) as monitored by EPR after 11 h (Figure 2), a time period in which no EPR signal is seen in the absence of added ligand anion (vida supra). Thus, autoreduction is accelerated 4–5-fold at $[N_3^-]/[\mu\text{-}S^{2-}\text{-met}] \sim 570$. The anaerobic reaction of $\mu$-$S^{2-}$met plus azide results in an absorption spectrum (not shown) with a broad peak at 470 nm and a shoulder at 340 nm. The shoulder at 340 nm is indicative of $\mu$-$S^{2-}$semi-met. Since the EPR spectra of this reaction show development of only the $\mu$-$S^{2-}$semi-met signal, formation of semi-met$N_3^-$ need not be considered. The broad peak at 470 nm is presumably due to $\mu$-$S^{2-}$semi-met containing ~15% met$N_3^-$. Other ligand anions also accelerate the anaerobic autoreduction of $\mu$-$S^{2-}$met in the order $N_3^- > CN^- \approx SCN^- > Cl^-$.

Addition of 1 equiv of $Fe(CN)_6^{3-}$ to $\mu$-$S^{2-}$met in $ClO_4^-$ under anaerobic conditions inhibits autoreduction. When the $\mu$-$S^{2-}$met control [no added $Fe(CN)_6^{3-}$] contains its maximum $\mu$-$S^{2-}$semi-met EPR signal (88 h), the $\mu$-$S^{2-}$met plus $Fe(CN)_6^{3-}$ solution is EPR silent. This inhibition of autoreduction by $Fe(CN)_6^{3-}$ can be explained as due to oxidations of both $S^{2-}$, which dissociates from $\mu$-$S^{2-}$met (reaction 2), and $\mu$-$S^{2-}$ semi-met, which may form via reaction 3.

*Reactivity of $\mu$-$S^{2-}$semi-met with $O_2$.* Freier et al. (1979) reported that the resonance Raman spectrum of $\mu$-$S^{2-}$semi-met was converted to that of oxyHr when $\mu$-$S^{2-}$semi-met was exposed to air. Monitoring by absorption and EPR spectra however, we obtain different results. The absorption spectrum of the reaction product of $\mu$-$S^{2-}$semi-met exposed to air consists of faint shoulders at approximately 320, 360, and 500 nm (Figure 3). Addition of $NaN_3$ results in the absorption spectrum of semi-met$N_3^-$ (Harrington et al., 1978; Wilkins & Harrington, 1983). Monitoring of the reaction by EPR confirms the presence of semi-met, but there are subtle differences depending on the presence or absence of perchlorate (Figures 4 and 5). $\mu$-$S^{2-}$semi-met must be exposed to air for at least 15 min in Tris–perchlorate before any change in the EPR signal is observed, whereas in Tris–acetate samples of $\mu$-$S^{2-}$semi-met frozen within 2 min after exposure to $O_2$ show changes in the EPR spectrum. At times much earlier than 40-min exposure of $\mu$-$S^{2-}$semi-met to $O_2$, the EPR spectra contain a significant contribution from the $\mu$-$S^{2-}$semi-met signal. The spectra after long reaction times have nearly the same $g$ values: (Figure 4c) 2.02, 1.95, 1.86, and 1.72; (Figure 5b) 2.02, 1.95, 1.86, and 1.71. The difference is the persistence of the prominent $g = 1.71$ feature in perchlorate (Figure 5) compared to its decrease in intensity in acetate (Figure 4). With the exception of the $g = 2.02$ feature, the products of reactions of $\mu$-$S^{2-}$semi-met with $O_2$ have EPR spectra very similar to those observed during the conversion of $(\text{semi-met})_O$ toward $(\text{semi-met})_R$ reported by Wilkins & Harrington (1983). For comparison purposes, we prepared $(\text{semi-met})_O$ by oxidation of deoxyHr with $Fe(CN)_6^{3-}$ in Tris–acetate. The conversion toward $(\text{semi-met})_R$ was then monitored by EPR (Figure 6). When $(\text{semi-met})_O$ is prepared in Tris–perchlorate in place of Tris–acetate, the same conversion toward $(\text{semi-met})_R$ occurs, but the spectrum obtained at 49 min in Figure 6 is not observed until ~120 min in Tris–perchlorate (spectra not shown). Comparisons of spectra in Figures 4b and 5b with those in Figure 6 show that the product upon oxidative loss of sulfide from $\mu$-$S^{2-}$semi-met generates a spectrum that resembles the 8-min spectrum during conversion of $(\text{semi-met})_O$

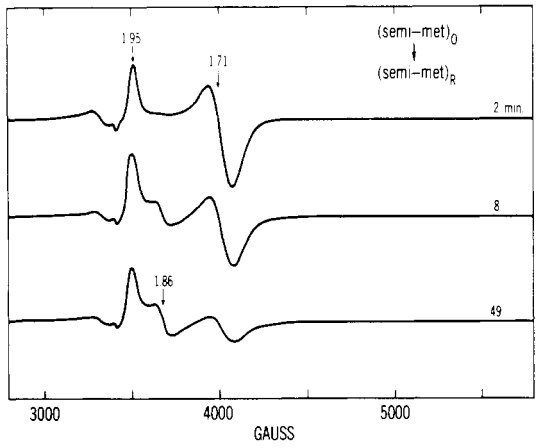


FIGURE 6: EPR spectra obtained during anaerobic incubation of (semi-met)$_O$ for the indicated times in 50 mM Tris–acetate, pH 8.0. EPR conditions are those listed in the legend to Figure 2 except the receiver gain is $6.3 \times 10^4$. The feature at ~3300 G is from the EPR cavity.

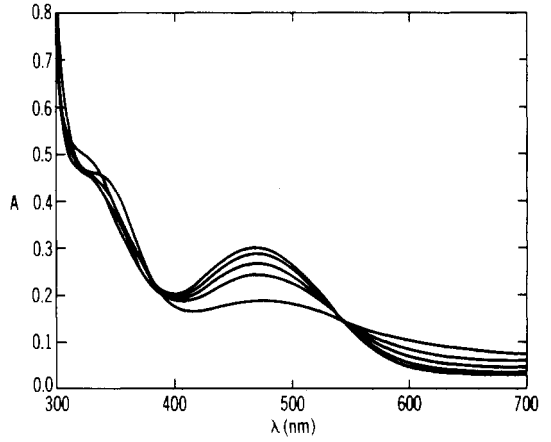


FIGURE 7: Absorption spectra obtained during aerobic incubation of 0.125 mM $\mu$-$S^{2-}$semi-met in 50 mM Tris–acetate, pH 8.0, at room temperature in the presence of 6.5 mM $NaN_3$. Excess sulfide was removed by passage over a Sephadex G-25 column. Cell path length = 1 cm. Reaction times (min) in order of increasing $A_{470}$ were 10, 25, 50, 115, and 295. The 295-min spectrum has highest $A_{320}$ and lowest $A_{600}$.

toward (semi-met)$_R$. Similar spectra are obtained at 40 min in Tris–acetate and 350 min in Tris–perchlorate. These reaction times are consistent with the slowing of the (semi-met)$_O$ → (semi-met)$_R$ conversion by perchlorate discussed above. A reasonable interpretation of these results is that (semi-met)$_O$ is the initial product upon oxidative loss of sulfide from $\mu$-$S^{2-}$semi-met and implies that $\mu$-$S^{2-}$semi-met is in a conformation resembling that of (semi-met)$_O$ when it loses sulfide oxidatively. The anaerobic loss of sulfide discussed above, which occurs over several days, can be interpreted as due to a slow conformational change of $\mu$-$S^{2-}$semi-met to one more prone to loss of sulfide, perhaps resembling that of (semi-met)$_R$.

We suspect that the results of Freier et al. (1979) discussed above are due to a photochemical reaction during laser irradiation of aerobic solutions of $\mu$-$S^{2-}$semi-met. We previously reported the bleaching of thawed solutions of $\mu$-$S^{2-}$met upon laser irradiation (Lukat et al., 1984). We have also found that prolonged laser irradiation of anaerobic solutions of $\mu$-$S^{2-}$semi-met results in formation of crystals of deoxyHr. The following series of reactions can explain the results of Freier et al. (1979):

$$\mu\text{-}S^{2-}\text{semi-met} \xrightarrow{h\nu} \text{(semi-met)}_O + S^{2-} \longrightarrow \text{deoxyHr} + \text{"}S^{-}\cdot\text{"}$$

$$\text{deoxyHr} \xrightarrow{O_2} \text{oxyHr}$$

We reported previously that (semi-met)$_O$ is rapidly reduced to deoxyHr by sulfide, whereas (semi-met)$_R$ forms $\mu$-$S^{2-}$semi-met (Lukat et al., 1984). The rapid photochemically induced release of relatively large amounts of $S^{2-}$ explains the formation of oxyHr rather than the thermal product, (semi-met)$_O$. Exchange of $O^{2-}$ in the $\mu$-oxo bridge of metmyoHr$N_3^-$ is also known to be light catalyzed (Duff et al., 1981).

The sharp $g = 2.02$ signal seen upon reaction of $\mu$-$S^{2-}$semi-met with $O_2$ (Figures 4 and 5) has power saturation behavior very different from that of any of the semi-metHr derivatives. Since passage over a Sephadex G-25 column does not eliminate the $g = 2.02$ signal, it must be associated with the protein. A similar EPR signal at $g = 2.01$ has been attributed to a cysteinyl disulfide radical (Cys–S–S·) generated during oxidation of [4Fe-4S] centers in *Azotobacter vinelandii* Fd I (Morgan et al., 1984). We have found that the $g = 2.02$ (but not the semi-met) signal disappears upon addition of dithiothreitol, ascorbate, or, as shown in Figures 4 and 5, $NaN_3$. The first two reagents most likely cause reduction of the radical with perhaps removal of (formally) $S^0$ in the case of dithiothreitol. Azide binding to metHr is known to greatly increase the rate of reaction of Cys-50 (the only Cys residue in *P. gouldii* Hr) with sulfhydryl reagents (Keresztes-Nagy & Klotz, 1965) and could destabilize the putative Cys–S–S· radical by, e.g., increasing its exposure to water.

As shown in Figures 3–5, addition of $N_3^-$ to the product of reaction of $\mu$-$S^{2-}$semi-met with $O_2$ results in formation of the characteristic UV–visible and EPR spectra of semi-met$N_3^-$ (Wilkins & Harrington, 1983). By either double integration of the EPR spectra or by using $\epsilon_{470} = 2400$ $M^{-1}$ $cm^{-1}$ for the absorption spectra, 90–100% of the initial protein concentration can be accounted for as semi-met$N_3^-$. Figure 7 shows optical spectra resulting from addition of excess $N_3^-$ to $\mu$-$S^{2-}$semi-met simultaneously with exposure to air. Two isosbestic points at ~544 and ~385 nm suggest that $\mu$-$S^{2-}$semi-met and semi-met$N_3^-$ are the only two species present. The transformation illustrated in Figure 7 can be explained in terms of the following two-step sequence:

$$4H^+ + O_2 + 2\mu\text{-}S^{2-}\text{semi-met} \rightarrow 2\text{(semi-met)}_{O,R} + 2S + 2H_2O \quad (4)$$

$$\text{(semi-met)}_{O,R} + N_3^- \rightleftarrows \text{semi-met}N_3^- \quad (5)$$

The formation constant for *P. gouldii* semi-met$N_3^-$ at pH 8.2 exceeds $10^3$ $M^{-1}$ $cm^{-1}$, and the half-life for reaction 3 should be a few seconds or less under our conditions (Harrington et al., 1978; Wilkins & Harrington, 1983). Thus, given the time course in Figure 3, the (semi-met)$_{O,R}$ intermediate should not be present in significant concentrations. EPR spectra obtained over the time course of the same reaction are also consistent with a mixture of only $\mu$-$S^{2-}$semi-met and semi-met$N_3^-$ as shown in spectra A and B of Figure 8. The simulations in Figure 8B indicate that ~60% semi-met$N_3^-$ is present after 15 min under the conditions used for Figure 8A. The similar time courses in Figures 5 and 8A, which were conducted with stirred samples open to air, suggest that $N_3^-$ does not significantly change the time course of reaction 4.

*Reactivity of $\mu$-$S^{2-}$met with $O_2$.* Previously, we reported on the aerobic decomposition of $\mu$-$S^{2-}$met in Tris–perchlorate (Lukat et al., 1984). When monitored by absorption spectroscopy, two isosbestic points are observed indicating the presence of only two species. Lack of an EPR signal

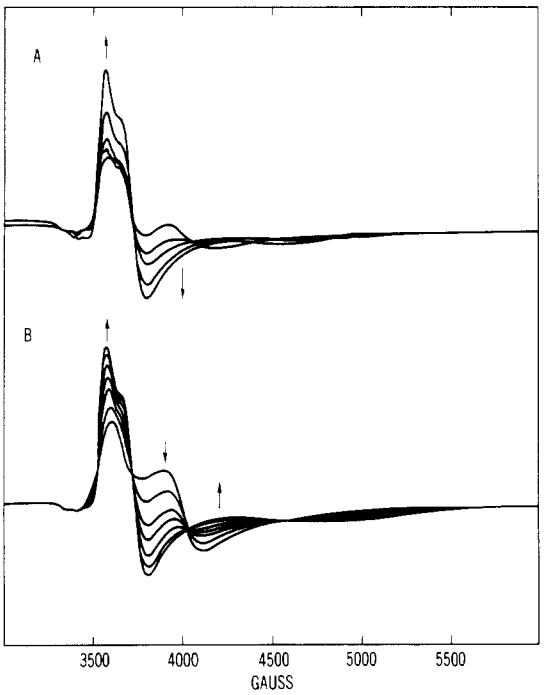


FIGURE 8: (A) EPR spectra obtained during aerobic incubation of 1.95 mM $\mu$-$S^{2-}$semi-met at room temperature in 50 mM Tris–perchlorate, pH 8.0, in the presence of 0.515 M $NaN_3^-$. Reaction times (min) in order of increasing intensity at the fields indicated by the vertical arrows are 15, 40, 63, 110, and 345. EPR conditions are those listed in the legend to Figure 5. (B) Computer simulation of EPR spectra resulting from mixtures of $\mu$-$S^{2-}$semi-met and semi-met$N_3^-$. Percentages of $\mu$-$S^{2-}$semi-met are 100, 75, 50, 35, 20, 8, and 0. Arrows indicate directions of decreasing $\mu$-$S^{2-}$semi-met content.

throughout the course of the reaction and formation of only met$N_3^-$ upon addition of azide suggest that $O_2$ is oxidizing the sulfide in a manner analogous to reaction 4:

$$4H^+ + 2\mu\text{-}S^{2-}\text{met} + O_2 \rightarrow 2\text{met} + 2H_2O + 2S \quad (6)$$

At $\sim$50 $\mu$M $\mu$-$S^{2-}$met, reaction 6 is complete in 12 h in Tris–perchlorate (Lukat et al., 1984). Thus, autoreduction (reactions 2 plus 3) is not observed during this time period. $\mu$-$S^{2-}$met is never exposed to significant concentrations of free sulfide in aerobic solutions because dissociation of sulfide (reaction 2) in Tris–perchlorate is not appreciable on the time scale of reaction 6. If $\mu$-$S^{2-}$met in Tris–acetate is exposed to $O_2$ in the absence of perchlorate, there is a slightly different result. During the reaction, two EPR-active species with $g$ values of 2.02 and 1.94, 1.88, and 1.71 are generated. These correspond to a signal that is very similar to ones observed during early times in the $\mu$-$S^{2-}$semi-met plus $O_2$ experiments discussed above. However, these semi-met signals account for no more than 6% of the total protein concentration. Apparently due to the faster rate of autoreduction of $\mu$-$S^{2-}$met in Tris–acetate than in Tris–perchlorate (Lukat et al., 1984), a minor pathway consisting of reactions 2–4 competes with the major pathway, reaction 6, which is the only one seen in Tris–perchlorate.

Previously, we reported that in Tris–acetate aerobic incubation of $\mu$-$S^{2-}$met with excess $N_3^-$ results in formation of the semi-met$N_3^-$ EPR signal (Lukat et al., 1984; see Added in Proof). However, aerobic incubation of $\mu$-$S^{2-}$met in Tris–perchlorate in the presence of a 267-fold molar excess of $NaN_3$, when followed by EPR (not shown), reveals a mixture containing $\sim$40% $\mu$-$S^{2-}$semi-met and $\sim$60% semi-met$N_3^-$ when the maximum EPR signal is obtained (365 min, 0.9 spin per two Fe). These results can be explained as an acceleration of autoreduction of $\mu$-$S^{2-}$met (reactions 2 and 3), by $N_3^-$ which suppresses reaction 6. The resulting $\mu$-$S^{2-}$semi-met then undergoes its usual aerobic reactions 4 and 5. The appearance of $\mu$-$S^{2-}$semi-met as an intermediate in Tris–perchlorate but not in Tris–acetate is consistent with the slowing of reaction 4 in Tris–perchlorate discussed above. At reaction times $\gtrsim$10 h, the aerobic solutions of $\mu$-$S^{2-}$met plus $N_3^-$ show decreased EPR intensities, and the optical spectra indicate conversion to met$N_3^-$.

*Reaction of DeoxyHr with Sulfide.* We have been unable to detect any reaction of $\mu$-$S^{2-}$semi-met with excess $Na_2S_2O_4$. If this lack of reaction is thermodynamically controlled, the $\mu$-$S^{2-}$semi-met $\rightarrow$ "$\mu$-$S^{2-}$deoxy" reduction potential must be quite negative. We have previously drawn the analogy to lack of reduction of [2Fe-2S] centers beyond the $Fe^{2+}Fe^{3+}$ level in ferredoxins (Lukat et al., 1984).

Binding of sulfide to the iron site of deoxyHr would be difficult to detect optically. However, Reem & Solomon (1985) recently discovered an EPR signal at $g$ = 13 due to a $N_3^-$ adduct of deoxyHr (deoxy$N_3^-$). They assigned this signal to a "forbidden" $M_s = \pm 2$ transition of an uncoupled high-spin $Fe^{2+}$. We have found that this EPR signal gradually disappears upon titration of deoxy$N_3^-$ with excess sulfide. These EPR spectra (included as Figure 9 in the supplementary material; see paragraph at end of paper regarding supplementary material) indicate a weak association of $S^{2-}$ with deoxyHr, since the formation constant for deoxy$N_3^-$ is estimated to be 70 $M^{-1}$ (Bradić et al., 1977). Disappearance of the $g$ = 13 EPR signal is consistent with magnetic coupling of the unpaired spins on the iron site. However, upon oxidation of deoxyHr in the presence of excess sulfide we have been able to obtain only metHr. Thus, the nature of the product of reaction of deoxyHr with sulfide remains unclear.

## CONCLUSIONS

Scheme I summarizes the results of this and other investigations. The most important new conclusions from the present work are as follows: (i) Replacement of bridging $O^{2-}$ by $S^{2-}$ results in an $\sim$200-mV positive shift in the met/semi-met reduction potential. (ii) The $\mu$-$S^{2-}$Hrs appear to exist in two conformers, one of which resembles $(\text{semi-met})_O$. (iii) Reactions of $\mu$-$S^{2-}$met and $\mu$-$S^{2-}$semi-met with $O_2$ are $S^{2-}$ based and result in conversion to metHr and $(\text{semi-met})_O$, respectively; $O_2$ appears to react with bound $S^{2-}$, since the reactions with $O_2$ are much faster than anaerobic dissociation of $S^{2-}$. (iv) Unlike $O_2$, ligand anions accelerate the autoreduction of $\mu$-$S^{2-}$met to $\mu$-$S^{2-}$semi-met. This acceleration causes the reaction of $\mu$-$S^{2-}$met with $O_2$ in the presence of $N_3^-$ to proceed through $\mu$-$S^{2-}$semi-met. (v) Perchlorate binding to the $\mu$-$S^{2-}$Hrs slows both oxidative loss of sulfide and autoreduction. (vi) $\mu$-$S^{2-}$semi-met cannot be reduced by $S_2O_4^{2-}$; however, $S^{2-}$ apparently does interact with deoxyHr.

Recently, Maroney et al. (1984) have provided evidence that the magnetic coupling between irons in semi-met$N_3^-$ is $\sim$ 10-fold weaker than that in met$N_3^-$. This result is consistent with a $\mu$-hydroxo bridge in semi-met rather than a $\mu$-oxo bridge as in met. A $\mu$-hydroxo bridge should be more labile and would explain our observation that $S^{2-}$ replaces the bridging ligand in semi-met- but not in metHr (Scheme I). Reem & Solomon (1984) have postulated the existence of a $\mu$-hydroxo bridge between iron atoms in deoxyHr in the absence of $N_3^-$.

Previously we suggested that the lack of formation of a stable azide adduct of $\mu$-$S^{2-}$met was due to generation of severe steric restrictions at the 5-coordinate iron upon replacement of the bridging $O^{2-}$ with the larger $S^{2-}$ (Lukat et al., 1984). More recent results suggest that the severe steric restrictions

are conserved at the semi-met oxidation level. Both met- and semi-metHr form stable azide adducts (Scheme I), whereas both $\mu$-$S^{2-}$met and $\mu$-$S^{2-}$semi-met do not. Although one could argue that the lack of azide binding to $\mu$-$S^{2-}$semi-met is due to reduction of the exposed iron, the fact that azide can bind to deoxyHr suggests that electronic factors alone do not prevent azide binding to $\mu$-$S^{2-}$semi-met.

*Comparisons to [2Fe-2S] Centers.* The $Fe_2S_2$ core of the [2Fe-2S] center in spinach ferredoxin is presumably attached to the protein exclusively via two terminal thiolate ligands per iron, and the $Fe_2S_2^{2+/1+}$ reduction potential is −420 mV vs. NHE (Berg & Holm, 1982). On the basis of electrostatic considerations, terminal ligation by neutral imidazoles rather than negatively charged thiolates should lead to a significant increase in this value. The $Fe_2S(O_2CR)_2^{2+/1+}$ reduction potential in $\mu$-$S^{2-}$Hr (283–312 mV) is in agreement with this expectation and falls within the range of the Rieske iron–sulfur centers (150–330 mV) (Malkin & Bearden, 1978; Bowyer et al., 1982). Apparently, these rather positive reduction potentials are responsible for the autoreduction of $\mu$-$S^{2-}$met as well as of at least one of the Rieske centers (Rieske et al., 1964). The analytical and Mössbauer data for the Rieske center from *Thermus thermophilus* are consistent with an $Fe_2S_2$ core and are significantly different from those of $\mu$-$S^{2-}$met (Fee et al., 1984; Lukat et al., 1984). Therefore, despite the resemblance in optical and EPR spectra, the center in $\mu$-$S^{2-}$Hr is apparently different from the Rieske center. However, on the basis of our data, it is not unreasonable to propose that histidine imidazoles provide some of the ligands to the iron atoms in the Rieske center. The amino acid composition of the Rieske protein from *T. thermophilus* requires that at least two terminal ligands per [2Fe-2S] center be other than cysteine thiolate and the histidine content would permit two imidazole ligands per center (Fee et al., 1984).

Finally, although we cannot yet attach any physiological significance to the sulfide binding properties of Hr, it is interesting to note that the bloods of a few other marine organisms, including the deep-sea hydrothermal vent tube worm *Riftia pachyptila*, have recently been reported to reversibly bind sulfide (Arp & Childress, 1983; Childress et al., 1984).

## Added in Proof

Our most recent spin quantitations of the semi-met$N_3^-$ EPR signal resulting from aerobic reaction of $\mu$-$S^{2-}$met with excess $N_3^-$ in Tris–acetate yield ~0.8 spin per two Fe.

## Supplementary Material Available

A figure with legend depicting titration of the deoxy$N_3^-$ EPR signal with excess sulfide (1 page). Ordering information is given on any current masthead page.

**Registry No.** Perchlorate, 14797-73-0; oxygen, 7782-44-7; azide, 14343-69-2; sulfide, 18496-25-8.

## References


Aasa, R., & Vänngard, T. (1975) *J. Magn. Reson. 19*, 308–315.

Armstrong, F. A., Harrington, P. C., & Wilkins, R. G. (1983) *J. Inorg. Biochem. 18*, 83–91.

Arp, A. J., & Childress, J. J. (1983) *Science (Washington, D.C.) 219*, 295–297.

Averill, B. A., Bale, J. R., & Orme-Johnson, W. H. (1978) *J. Am. Chem. Soc. 100*, 3034–3043.

Babcock, L. M., Bradič, Z., Harrington, P. C., Wilkins, R. G., & Yoneda, G. S. (1980) *J. Am. Chem. Soc. 102*, 2849–2850.

Berg, J. M., & Holm, R. H. (1982) in *Iron-Sulfur Proteins* (Spiro, T. G., Ed.) pp 1–66, Wiley, New York.

Bowyer, J. R., Edwards, C. A., Ohnishi, T., & Trumpower, B. L. (1982) *J. Biol. Chem. 257*, 8321–8330.

Bradič, Z., & Wilkins, R. G. (1983) *Biochemistry 22*, 5396–5401.

Bradič, Z., Conrad, R., & Wilkins, R. G. (1977) *J. Biol. Chem. 252*, 6069–6075.

Bradič, Z., Harrington, P. C., Wilkins, R. G., & Yoneda, G. (1980) *Biochemistry 19*, 4149–4155.

Burkey, K. O., & Gross, E. L. (1982) *Biochemistry 21*, 5886–5890.

Childress, J. J., Arp, A. J., & Fisher, C. R., Jr. (1984) *Mar. Biol. (Berlin) 83*, 109–124.

Darnall, D. W., Garbett, K., & Klotz, I. M. (1968) *Biochem. Biophys. Res. Commun. 32*, 264–271.

Dawson, J. W., Gray, H. B., Hoenig, H. E., Rossman, G. R., Schredder, J. M., & Wang, R. H. (1972) *Biochemistry 11*, 461–465.

Duff, L. L., Klippenstein, G. L., Shriver, D. F., & Klotz, I. M. (1981) *Proc. Natl. Acad. Sci. U.S.A. 78*, 4138–4140.

Dutton, P. L., & Wilson, D. F. (1974) *Biochim. Biophys. Acta 346*, 165–212.

Fee, J. A., Findling, K. L., Yoshida, T., Hille, R., Tan, G. E., Hearshen, D. O., Dunham, W. R., Day, E. P., Kent, T. P., & Münck, E. (1984) *J. Biol. Chem. 259*, 124–133.

Freier, S. M., Duff, L. L., VanDuyne, R. P., & Klotz, I. M. (1979) *Biochemistry 18*, 5372–5377.

Garbett, K., Darnall, D. W., & Klotz, I. M. (1971a) *Arch. Biochem. Biophys. 142*, 471–480.

Garbett, K., Darnall, D. W., & Klotz, I. M. (1971b) *Arch. Biochem. Biophys. 142*, 455–470.

Harrington, P. C., deWaal, D. J. A., & Wilkins, R. G. (1978) *Arch. Biochem. Biophys. 191*, 444–451.

Harrington, P. C., Wilkins, R. G., Muhoberac, B. B., & Wharton, D. C. (1982) in *The Biological Chemistry of Iron* (Dunford, H. B., Dolphin, D., Raymond, K. N., & Sieker, L., Eds.) pp 145–160, Reidel, Dordrecht, Holland.

Heineman, W. R., Norris, B. J., & Goelz, J. F. (1975) *Anal. Chem. 47*, 79–84.

Irwin, M. J., Duff, L. L., Shriver, D. F., & Klotz, I. M. (1983) *Arch. Biochem. Biophys. 224*, 473–478.

Keresztes-Nagy, S., & Klotz, I. M. (1965) *Biochemistry 4*, 919–931.

Klotz, I. M., & Kurtz, D. M., Jr. (1984) *Acc. Chem. Res. 17*, 16–22.

Klotz, I. M., Klotz, T. A., & Fiess, H. A. (1957) *Arch. Biochim. Biophys. 68*, 284–299.

Krueger, R. J., & Siegel, L. M. (1982) *Biochemistry 21*, 2892–2904.

Kurtz, D. M., Jr., Shriver, D. F., & Klotz, I. M. (1977) *Coord. Chem. Rev. 24*, 145–178.

Kurtz, D. M., Jr., Sage, J. T., Hendrich, M., Debrunner, P. G., & Lukat, G. S. (1983) *J. Biol. Chem. 258*, 2115–2117.

Lukat, G. S., Kurtz, D. M., Jr., Shiemke, A. K., Loehr, T. M., & Sanders-Loehr, J. (1984) *Biochemistry 23*, 6416–6422.

Malkin, R., & Bearden, A. J. (1978) *Biochim. Biophys. Acta 505*, 147–181.

Margalit, R., & Schejter, A. (1973) *Eur. J. Biochem. 32*, 492–499.

Margoliash, E., & Frohwirt, N. (1959) *Biochem. J. 71*, 570–572.

Margoliash, E., & Walasek, O. F. (1967) *Methods Enzymol. 10*, 339–348.

Maroney, M. J., Lauffer, R. B., Que, L., Jr., & Kurtz, D. M., Jr. (1984) *J. Am. Chem. Soc. 106*, 6445-6446.
Morgan, T. V., Stephens, P. J., Derlin, F., Stout, C. D., Melis, K. A., & Burgess, B. K. (1984) *Proc. Natl. Acad. Sci. U.S.A. 81*, 1931-1935.
Muhoberac, B. B., Wharton, D. C., Babcock, L. M., Harrington, P. C., & Wilkins, R. G. (1980) *Biochim. Biophys. Acta 626*, 337-345.
O'Reilly, J. E. (1973) *Biochim. Biophys. Acta 292*, 509-515.
Reem, R. C., & Solomon, E. I. (1984) *J. Am. Chem. Soc. 106*, 8323-8325.
Reiske, J. S., Hansen, R. E., & Zaugg, W. S. (1964) *J. Biol. Chem. 239*, 3017-3022.
Sanders-Loehr, J., & Loehr, T. M. (1979) *Adv. Inorg. Biochem. 1*, 235-252.
Stenkamp, R. E., Sieker, L. C., & Jensen, L. H. (1978) *J. Mol. Biol. 126*, 457-466.
Stenkamp, R. E., Sieker, L. C., & Jensen, L. H. (1983) *J. Inorg. Biochem. 19*, 247-253.
Stenkamp, R. E., Sieker, L. C., & Jensen, L. H. (1984) *J. Am. Chem. Soc. 106*, 618-622.
Stenkamp, R. E., Sieker, L. C., Jensen, L. H., McCallum, J. D., & Sanders-Loehr, J. (1985) *Proc. Natl. Acad. Sci. U.S.A. 82*, 713-716.
Wilkins, R. G., & Harrington, P. C. (1983) *Adv. Inorg. Biochem. 5*, 51-85.

# Release of Iron from the Two Iron-Binding Sites of Transferrin by Cultured Human Cells: Modulation by Methylamine†

Adrian Bomford,* Stephen P. Young,‡ and Roger Williams
*The Liver Unit, School of Medicine and Dentistry of King's College London, London SE5 8RX, U.K.*
*Received September 19, 1984*

ABSTRACT: We have investigated the effect of increasing concentrations of methylamine (5, 10, and 25 mM) on the removal of iron from the two iron-binding sites of transferrin during endocytosis by human erythroleukemia (K562) cells. The molecular forms of transferrin released from the cells were analyzed by polyacrylamide gel electrophoresis in 6 M urea. Endocytosis of diferric transferrin was efficient since <10% of surface-bound protein escaped endocytosis and was released in the diferric form. Although transferrin exocytosed from control cells had been depleted of 80% of its iron and contained 65-70% apotransferrin, iron-bearing species were also released (15% C-terminal monoferric; 10% N-terminal; 10% diferric). The ratio of the two monoferric species (C/N) was 1.32 ± 0.12 (mean ± SD; $n = 4$), suggesting that iron in the N-terminal site was more accessible to cells. In the presence of methylamine there was a concentration-dependent increase in the proportion of diferric transferrin release (>80% at 25 mM) and a concomitant decrease in apotransferrin. Small amounts of the iron-depleted species, especially apotransferrin, appeared before diferric transferrin, suggesting that these were preferentially released from the cells. The discrepancy between the proportions of the monoferric transferrin species noted with control cells was enhanced at all concentrations of methylamine, most markedly at 10 mM when the C/N ratio was 2.4. The N-terminal site of transferrin loses its iron at a higher pH than the C-terminal site, and so by progressively perturbing the pH of the endocytic vesicle we have increased the difference between the two sites observed with control cells. The observation that the in vitro site differences apply during interaction of transferrin with cells suggests that protonation of the sites is of prime importance in iron release.

The plasma iron-transport glycoprotein transferrin consists of a single polypeptide chain ($M_r$ 80000) bearing two specific binding sites that can each bind an atom of iron with high affinity (Morgan, 1974). Because the binding of iron to transferrin displaces protons from the protein, the equilibrium can be perturbed by lowering the pH, and this method has been widely used to remove iron from transferrin during studies of the protein-metal interaction (Lestas, 1976; Princiotto & Zapolski, 1975; Aisen et al., 1978). Similarly, reductive removal of iron from transferrin can be achieved since Fe(II) is only weakly bound (Gaber & Aisen, 1970), but this only occurs rapidly if an agent to displace the coanion bicarbonate from the protein-iron complex is present (Ankel & Petering, 1980). Thus two nondestructive methods are available to overcome the kinetic barrier to the release of iron from the transferrin, and it seems likely that cells make use of one or both of these methods to remove the iron. Some evidence suggests that transferrin iron becomes available to chelators of Fe(II) within the cell and therefore passes through a stage at which it is reduced (Morgan, 1971; Thorstensen & Romslo, 1984), and it is now realized that the protein encounters an environment at low pH during its transit through the cell. However, a more definitive conclusion on the relative importance for cellular acquisition of iron of reduction and protonation is not yet possible.

The initial event in cellular iron uptake involves the binding of iron-rich transferrin to specific cell-surface receptors that are found on erythroid cells (Jandl & Katz, 1963; Iacopetta & Morgan, 1983), normal nonerythroid cells (Young & Aisen, 1980; Galbraith et al., 1980; Hamilton et al., 1984), and a wide variety of cultured cell lines (Seligman, 1983). Some workers have interpreted data on the binding and release of transferrin from cells (Woodworth et al., 1982) and on the accessibility of iron to chelating agents during uptake from transferrin (Nunez et al., 1983; Nunez & Glass, 1983) as indicating that

† This work was supported in part by a grant from the Medical Research Council.
‡ Present address: Department of Rheumatology, The University of Birmingham, Birmingham B15 2TJ, U.K.

0006-2960/85/0424-3472$01.50/0 